The Development and Validation of a Tactical Grade EGI System for Land Vehicular Navigation Applications

Y.-E. Huang [1]*, S. Tsai [1], H.-Y. Liu[1], K.-W. Chiang[2], M.-L. Tsai[2], P.-L. Lee[2], N. El-Sheimy[3]

[1] Department of Geomatics, National Cheng Kung University, Taiwan – (jimmy4345, dino920135, qwerim101117) @gmail.com
[2] Department of Geomatics, National Cheng Kung University, Taiwan – (kwchiang, taurusbryant, pointpl) @geomatics.ncku.edu.tw
[3] Dept. of Geomatics Engineering, University of Calgary, 2500 University Dr NW, Calgary, AB T2N 1N4, Canada – (elsheimy)@ucalgary.ca

KEY WORDS: Extended Kalman Filter, Tactical-grade Embedded GNSS/INS System, GNSS challenges, Initial Alignment, Time Synchronization.

ABSTRACT:

Over recent years, the utilization of commercially available integrated navigation systems for the development of navigation algorithms has become increasingly commonplace. Nevertheless, the wide range of sensor quality on the market complicates system customization and restricts the evolution of navigation algorithms. This study aims to address these issues by creating an affordable, tactical-grade, real-time integrated navigation system, EGI-500 (Embedded GNSS and INS), encompassing both hardware and software components. EGI-500 incorporates a tactical-grade IMU500 and a Septentrio Mosaic-X5 GNSS receiver module. The integration process is segmented into three distinct stages. The first involves hardware integration, with an illustrative architecture diagram of the real-time navigation system. Second, we focus on data preprocessing, where a cross-correlation approach is proposed to tackle multi-sensor time synchronization issues, specifically to determine potential time lags in IMU data. The final phase covers the fusion of multi-sensor data and motion constraints. The Extended Kalman Filter (EKF) forms the backbone of this part, with Zero Velocity Update (ZUPT) and Non-Holonomic Constraints (NHC) being integrated into the Loosely Coupled (LC) scheme. Furthermore, the IMU calibration process is performed to ascertain necessary algorithmic parameters. Experimental results, conducted in diverse environments (open sky, GNSS challenging, and GNSS denied), will be presented in this paper. Comparisons with reference data indicate that the navigation accuracy of the developed integrated system, both in terms of hardware and navigation algorithm, achieves expected meter-level accuracy, fulfilling the "Which Lane" and "Which Road" level criteria in varied environments. Furthermore, outcomes from the GNSS denied environment align with predictions based on propagation error theory, demonstrating the feasibility of our navigation algorithm for tactical integrated navigation systems.

1. INTRODUCTION

Navigational processes, which calculate the position, velocity, and attitude of a moving entity, are fundamental in Land Vehicular navigation (LVN). Primarily, the Global Navigation Satellite System (GNSS) has become the go-to method for navigation. However, in challenging or GNSS obstructed settings, GNSS receivers fail to secure any signal. This has led to the increasing importance of the Inertial Navigation System (INS), which is often amalgamated with GNSS due to their cooperative attributes. Though navigation-grade IMUs provide a high degree of accuracy, they come with a hefty price tag. On the other hand, consumer-grade IMUs, though affordable, offer limited advantages towards achieving high precision (Petovello, M. G., 2003). To approach for high navigational accuracy across a range of environments while maintaining cost-effectiveness, this research therefore proposes substituting navigation-grade IMUs with tactical-grade counterparts. The commencement of this integrative process requires hardware integration of the GNSS receiver module and IMU, one of the primary obstacles being the time synchronization between GNSS receiver and IMU sampling (Skog, I., & Handel, P., 2008). Effectively addressing this issue is a vital step in creating a navigation system's hardware integration. For IMU data, it's essential to account for biases and scale factor errors. Accurate calibration can lead to significant enhancements in navigation outcomes (Ferguson, J., 2015). Moreover, precise estimation of parameters in error models is a prerequisite to navigation using Allan variance test. This is an efficient tool for estimating parameters of the INS error model. Concerning software integration, initial alignment, the process of obtaining the initial rotation angle, must be conducted before initiating navigation. Depending on the IMU used, different time thresholds must be established, underscoring the importance of identifying appropriate thresholds. While the Extended Kalman Filter (EKF) is a commonly used method to amalgamate IMU and GNSS data and this study focuses on employing loosely coupled integration methodologies. The functional safety emerges as the most critical, specifically the accurate provision of positioning and navigation data. **Figure 1** depicts the categorization of navigation accuracy. These four defined categories represent the degree of precision necessary for diverse Intelligent Transportation System (ITS) applications (Stephenson et al. 2011).

Of the various factors mentioned above, this study aims to focus on the development of a bespoke, tactical-grade embedded EGI system (EGI-500). This comprehensive system comprises a core algorithm, hardware integration, and data storage, all designed to satisfy the critical requirements of a LVN application. Concurrently, the system aspires to accomplish satisfactory performance levels, specifically "Which Lane" and "Which Road" levels and will undergo practical driving tests to verify the functionality and integrity of the embedded EGI system. Within this research, we will detail the specifications of the tactical-grade embedded EGI system (EGI-500), in addition to elaborating on the architecture of the hardware integration and the core fusion algorithm. A methodology to validate the effectiveness of the hardware integration will also be provided. Furthermore, the accuracy of the tactical-grade embedded EGI system (EGI-500) will be assessed and presented based on the outcomes of a real-world road test.

The key contributions of this study can be enumerated as follows:

1. Development of a hardware integration framework, tailored specifically for embedded GNSS/INS systems in terrestrial vehicular navigation.
2. Introduction of a novel navigation integration algorithm, designed with an emphasis on tactical-grade IMUs and GNSS receivers within the context of embedded GNSS/INS systems for land-based vehicular navigation.
3. Proposal of an innovative method and a sequence of steps for validating the effectiveness of the hardware integration and navigation integration algorithm.

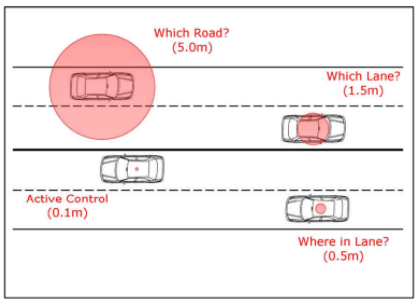

Figure 1. Navigation accuracy classification

The organization of this paper is as follows: Section 1 provides an introductory overview. The methods employed to achieve the integrated navigation system are elaborated in Section 2. The setup for the experiments conducted within this research is outlined in Section 3. Following this, Section 4 presents the findings of the real-time integrated navigation system EGI-500. Finally, a summary and conclusion are drawn in Section 5.

2. TACTICAL-GRADE EGI SYSTEM FRAMEWORK

In the ensuing segment, we present the overarching framework for the Tactical-grade EGI system. This comprehensive framework encompasses not only the creation but also the validation of both hardware and software components. The progression of the EGI system development is segmented into four fundamental stages:

1. Integration of Hardware Components.
2. Methodology for Time Synchronization Detection.
3. Calibration Process for the EGI System.
4. Algorithm Integration.

2.1 Hardware integration

In the field of hardware integration, our team has undertaken the development of an advanced real-time integrated navigation system featuring a tactical-grade specification. As depicted in **Figure 2**, the constituents of the system include a tactical-grade Inertial Measurement Unit (IMU), a Global Navigation Satellite System (GNSS) receiver module, a Real-Time Clock (RTC), a microcontroller, and an Industrial Personal Computer (IPC). Our research implemented the IMU500, renowned for its bias instability of merely 0.3 degrees per hour and a rapid sampling rate of 200 Hz, as the inertial sensor within the EGI-500. As the GNSS receiver module, the Septentrio Mosaic-X5 was preferred, with its sampling rate set at 1 Hz. A crucial aspect of our work focused on the time synchronization process, which was completed using the EPSON RX8900SA, a RTC chip. This chip is distinguished by its dependable stability and high-frequency operation. Upon acquiring a GNSS signal, the GNSS receiver module initiates the Pulse Per Second (PPS) signal and the GNSS solution. This first action sets the RTC to the existing GPST and initiates precise time calculation. Concurrently, the microcontroller (MCU) associates the GPST timestamp, provided by the RTC chip, with the IMU data. The final decision regarding the completion of time synchronization is determined by the MCU, which then dispatches both GNSS and IMU data, timestamped with GPST, to the IPC. The IPC, serving as the central pillar of our hardware integration architecture, is designed to enable complete standalone operation, devoid of supplementary computer connections. The chosen module, the NXP i.MX8, which incorporates an ARM Cortex architecture processor, is currently popular among automobile manufacturers for its ability to operate efficiently under extreme conditions like high temperatures and humidity. In the IPC, we've integrated an Embedded Multimedia Card (eMMC), an embedded flash memory. The Linux system and the real-time navigation algorithm are installed on this chip. Furthermore, to facilitate communication with external computers, Ethernet, and Universal Asynchronous Receiver/Transmitter (UART) transmission methods were designed into the IPC. With the hardware integration completed through our research, IMU data, including the GPST timestamp and the GNSS PVT solution signal, can be continually acquired. The comprehensive architecture of our hardware integration is illustrated in **Figure 3**.

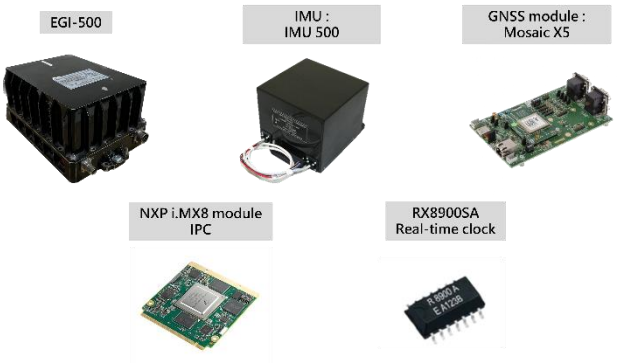

Figure 2. Main components in EGI-500

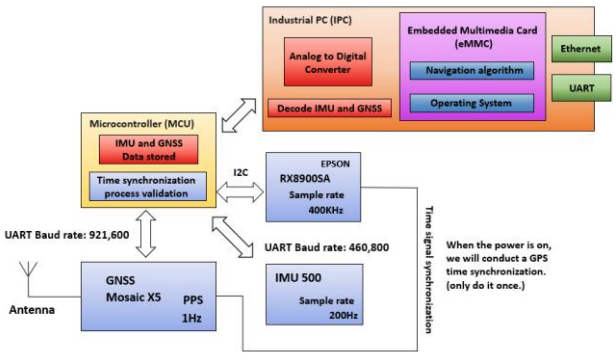

Figure 3. Hardware integration architecture.

2.2 Time Synchronization Detection Method

The question of time synchronization carries paramount significance during the initial phases of hardware integration. Any inaccuracies in the time information within the hardware can potentially propagate and magnify errors when fed into the navigation algorithm. Therefore, in this study, we have proposed a method for detecting time synchronization. This methodology aims to ascertain any delays in the timestamp of the IMU data. To implement this method, we utilized an IMU of the same

category, the iMAR-iNAV-RQH-10018, as the reference system. The timestamp of the reference system, viewed as the ground truth, is then compared to our IMU500. Given the discrepancy in the sampling rates between the reference system and the IMU500, we employed interpolation. Capitalizing on the distinct features of the IMU measurement signal, we calculated the value of cross-correlation at different time intervals. This information about the delay time aids us in fine-tuning the hardware integration architecture. In **Figure 4**, a case of zero-time delay is represented, indicating successful time synchronization. This is verified as the value derived from cross-correlation peaks at zero. If there are errors, the maximum value would occur in other regions. The equation that describes the method we proposed is as follows:

$$Value^{(Ref,\ IMU500)}{}_{Cross-correlation}(\mathrm{n}) = \frac{1}{n} * \sum_{i=0}^{n-1} IMU\ Measurement^{(Ref)}(i) IMU\ Measurement^{(IMU500)}(i+n) \quad (1)$$

where i = timestamp of IMU measurement
n = quantity of interpolated data

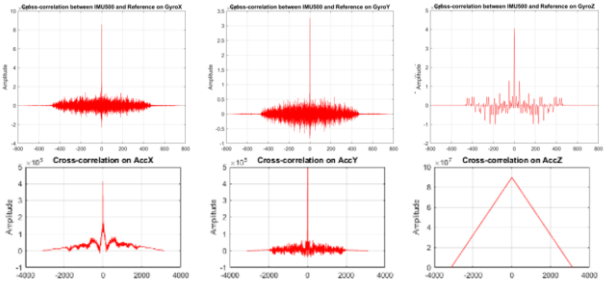

Figure 4. The illustrations of cross-correlation test results

2.3 Calibration of EGI System

To approximate the systematic error originating from the EGI-500, we estimate the bias and scale factor value on the side of accelerometers through a process of static calibration. For gyroscopes, we've employed a high-precision rotating table, EVO-20M, to carry out the calibration procedure as illustrated in **Figure 5**. The specifications of EVO-20M are detailed in **Table 1**. Leveraging both static and dynamic calibration, the bias and scale factor are input into the navigation algorithm. This step aids in mitigating the systematic error of the IMU and facilitates the construction of the error model.

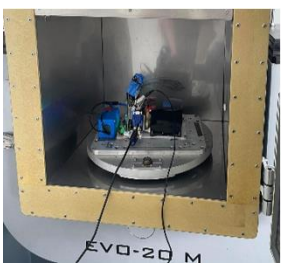

Figure 5. Dynamic calibration of EGI-500

Table 1. Specification of EVO-20M

Position accuracy	≤ ±1 arc sec
Maximum wobble	≤ 1 arc sec
Orthogonality	≤ 2 arc sec
Maximum rate	3000 °/s
Peak acceleration	2000 °/s²
Bandwidth	100 Hz

Additionally, both random and systematic noise constitute the primary sources of error within the navigation system. An accurate error model, predicated on these elements, needs to be constructed prior to utilizing IMU measurements. Typically, the parameters for the error model can be located on the official website or within the user manual. However, post-production or shipping from the original manufacturer can lead to inconsistencies between the IMU's specifications and the official parameters. Since IMU 500 also a Fiber Optic Gyroscopes (FOG), which can cause non-stationary behaviour due to intense vibrations, rapid rotation, and temperature increases, it is crucial to develop a model that accommodates the time-dependent stability of FOGs (Wang et al. 2015). Thus, we've adopted the Allan variance test to estimate parameters of the error model, such as the Angular Random Walk (ARW), Velocity Random Walk (VRW), and bias instability for accelerometers and gyroscopes. A comparison of the parameters from the user manual and those derived from the Allan variance test can be found in **Table 2**.

Table 2. Parameters of error model from the official document and Allan variance test

Error model	Specifications (IMU 500)	Allan variance (EGI-500)
	Gyroscope	
Bias Instability	0.3 (deg/hour)	0.01 (deg/hour)
Angular random walk	0.007 (deg/√hour)	0.005 (deg/√hour)
	Accelerometers	
Bias Instability	20 (μg)	17 (μg)
Velocity random walk	0.05 ((m/sec)/√hour)	0.0292 ((m/sec)/√hour)

2.4 Integrated Algorithm

In our study, we employ the EKF to fuse the data sourced from the IMU and the GNSS receiver module. The EKF is a universally adopted technique for INS and GNSS integration. It utilizes a Taylor series expansion under the presumption of Gaussian error distribution. Moreover, in an EKF framework, prediction and measurement updates are performed in a sequential manner (El-Sheimy et al., 2007). The simplicity of the LC scheme has led to its widespread adoption in the integration of multiple sensors for navigation. Consequently, in our research, we have chosen the LC method based as our fusion architecture, as illustrated in **Figure 6**.

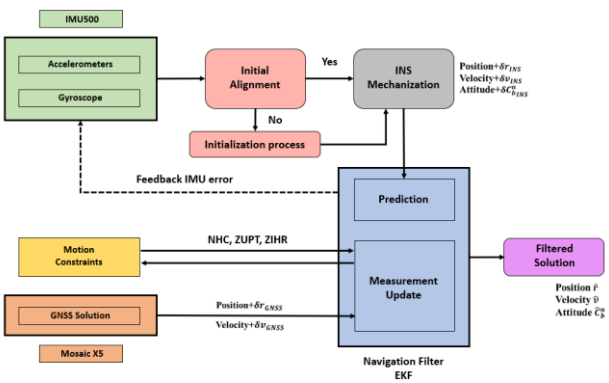

Figure 6. Loosely coupled based integration architecture

2.4.1 Initial Alignment

The primary foundation of an inertial navigation system hinges on IMU measurements. Prior to integrating IMU and GNSS data for navigation, it is imperative to transform the IMU measurements from the body frame to the navigation frame. This transformation process is termed as initial alignment. As tactical-grade IMUs can sense earth's rotation, initial alignment can be performed utilizing earth rotation measurements once the initial position has been obtained from the GNSS solution. This process comprises of two stages: coarse alignment and fine alignment, the flowchart for which is depicted in **Figure 7**.

During coarse alignment, we first calculate the mean value of a series of IMU measurements. Subsequently, we establish the ideal measurements in the navigation frame while in a static state. Having measurements in both body and navigation frames allows us to obtain the initial rotation angles. The equation for coarse alignment is expressed as follows:

$$\begin{bmatrix} f^b \\ \omega_{ib}^b \\ v^b \end{bmatrix} = C_n^b \times \begin{bmatrix} f^n \\ \omega_{ib}^n \\ v^n \end{bmatrix} \quad (2)$$

$$C_b^n = \begin{bmatrix} (f^n)^T \\ (\omega_{ib}^n)^T \\ (v^n)^T \end{bmatrix}^{-1} \times \begin{bmatrix} (f^b)^T \\ (\omega_{ib}^b)^T \\ (v^b)^T \end{bmatrix} \quad (3)$$

$$\begin{bmatrix} (f^n)^T \\ (\omega_{ib}^n)^T \\ (v^n)^T \end{bmatrix}^{-1} = \begin{bmatrix} 0 & 0 & -\gamma \\ \omega_e & 0 & -\omega_e sin\varphi \\ 0 & -\gamma\omega_e cos\varphi & 0 \end{bmatrix} \quad (4)$$

where f^b, f^n represent the specific force in the b-frame and n-frame respectively, ω_{ib}^b, ω_{in}^n represent the angular rate in the b-frame and n-frame respectively, v^b, v^n are the cross products of specific force and angular rate in the b-frame and n-frame respectively, C_n^b and C_b^n are rotation matrices from the n-frame to b-frame and b-frame to n-frame respectively, ω_e represents the earth rotation rate, γ represents the normal gravity, φ represents the latitude.

For fine alignment, we leverage the Extended Kalman Filter (EKF) to obtain a more precise initial rotation matrix from the body frame to the navigation frame. Two measurements are used for updating: the zero velocity, and the east channel earth rotation vector. The equations for Zero Velocity Update (ZUPT) and East Channel Earth Rotation Update (ECERU) are given below:

$$Z_{ZUPT} = [v_{ins}^n - 0_{3\times1}]_{3\times1} \quad (5)$$

$$H_{ZUPT} = [0_{3\times3} \quad I_{3\times3} \quad 0_{3\times15}]_{3\times21} \quad (6)$$

$$Z_{ECERU} = \left[C_b^n(2,1) \times \omega_x + C_b^n(2,2) \times \omega_y + C_b^n(2,3) \times \omega_y\right]_{1\times1} \times \frac{1}{Sampling\ rate} \times 180/pi \quad (7)$$

$$H_{ECERU} = \begin{bmatrix} 0_{1\times6} \\ \omega_{ie}^n(3,1) \\ 0 \\ -\omega_{ie}^n(1,1) \\ C_b^n(2,1) \\ C_b^n(2,2) \\ C_b^n(2,3) \\ 0_{1\times9} \end{bmatrix}_{1\times21} \quad (8)$$

where v_{ins}^n is the estimated velocity in the navigation frame, Z_{ZUPT} is the observation matrix, H_{ZUPT} is the design matrix, ω is the angular rate of the IMU, ω_{ie}^n is the rotation rate from the inertial frame to the earth frame under the navigation frame.

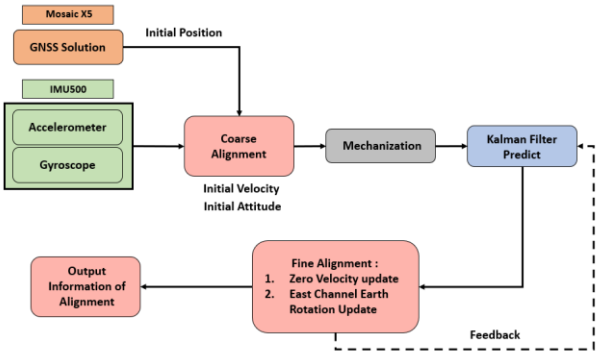

Figure 7. Flow chart of initial alignment

2.4.2 GNSS Update

When the GNSS receiver is able to acquire signals from at least four satellites, it can compute its coordinates. Consequently, we can carry out Coordinate Update (CUPT) based on the GNSS solution. The equation representing the GNSS CUPT is formulated as follows:

$$Z_{CUPT} = \begin{bmatrix} r_{INS_N}^n - r_{GNSS_N}^n \\ r_{INS_E}^n - r_{GNSS_E}^n \\ r_{INS_D}^n - r_{GNSS_D}^n \end{bmatrix}_{3\times1} \quad (9)$$

$$H_{CUPT} = [I_{3\times3} \quad 0_{3\times3} \quad A_{CUPT} \quad 0_{3\times12}]_{3\times21} \quad (10)$$

$$R_{CUPT} = \begin{bmatrix} \sigma_N^2 & 0 & 0 \\ 0 & \sigma_E^2 & 0 \\ 0 & 0 & \sigma_D^2 \end{bmatrix} \quad (11)$$

where N, E, D stand for North, East, and Down in the local-level frame, r_{INS}^n represents the estimated position, r_{GNSS}^n is the position derived from the GNSS solution, σ is the standard deviation present in the GNSS data.

2.4.3 Motion Constraints

The navigation error can be constrained under certain conditions using motion constraints such as Non-Holonomic Constraints (NHC), Zero Velocity Update (ZUPT), and Zero Integrated Heading Rate (ZIHR). For NHC, we assume that the velocity in the plane orthogonal to the forward direction is nearly zero, except in instances where the vehicle is sliding on a slope or airborne. This assumption can be applied for the update in EKF. The representation of this assumption is as follows:

$$v_y^b \approx 0, and\ v_z^b \approx 0 \quad (12)$$

where v_y^b, v_z^b represent velocities in the plane orthogonal to the forward direction in the body-frame.

The explanation and equations relating to ZUPT were already detailed in Section 2.4.1, hence it will not be reiterated in this section. Regarding ZIHR, it is assumed that the vehicle's rotation rate of the heading angle will be zero when the vehicle is stationary. Consequently, the heading angle value prior to the

vehicle becoming stationary can be utilized for measurement updates in EKF, thereby enhancing the accuracy of navigation.

$$Z_{ZIHR} = \left[\hat{\psi} - \psi\right]_{1\times1} \tag{13}$$

$$H_{ZIHR} = \left[0_{1\times10} \quad \frac{\sin\phi}{\cos\theta}\Delta t \quad \frac{\cos\phi}{\cos\theta}\Delta t \quad 0_{1\times9}\right]_{1\times21} \tag{14}$$

where $\hat{\psi}$ is the heading angle value, ψ, ϕ, θ are the stored values of heading angle, roll angle, and pitch angle, respectively, when the vehicle starts to become stationary, Δt is the time interval to verify whether the ZIHR can be conducted.

3. EXPERIMENT

In the context of this study, we employ a ground vehicle as a testbed to evaluate the real-time operational capability of the inertial navigation system EGI-500. In order to validate the viability of the proposed hardware architecture and navigation algorithm, we conduct experiments in three distinct settings: open sky, GNSS challenging environments, and GNSS denied scenarios, as depicted in **Figure 8**. To set up a reference system, we employ the Novatel PwrPak 7D-E2 for GNSS data acquisition, and the navigation-grade IMU, iMAR-iNAV-RQH-10018, for IMU data collection. We utilize the widely recognized commercial INS/GNSS software, Inertial Explorer (IE), to compute the reference trajectory. For the antenna part, the 72GNSSA-XT-1 antcom GNSS antenna is chosen for this research. **Table 3** provides a detailed specification of the IMU within the reference system, while **Figure 9** displays the experimental setup.

Figure 8. Three types of scenarios in road experiment

Table 3. Specification of iMAR-iNAV-RQH-10018

Gyroscope	
Bias Instability	0.002 (deg/hour)
Angular random walk	0.0015 (deg/√hour)
Accelerometers	
Bias Instability	10 (μg)
Velocity random walk	8 (μg/√Hz)

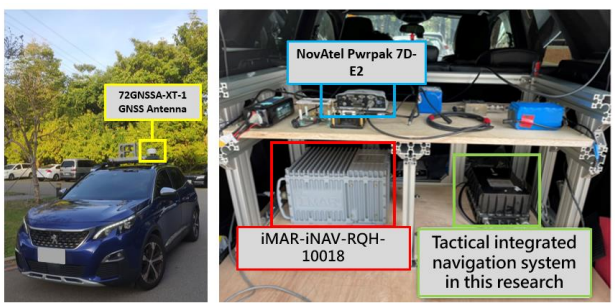

Figure 9. Device in the car experiment

4. RESULT AND DISCUSSION

4.1 Open Sky Experiment

The open-sky experiment was conducted along a stretch of a national highway, spanning approximately 41 km, with the vehicle speed maintained between 90 and 110 km/h. In this experiment, the GNSS solution operated in Single Point Positioning (SPP) mode. Given the SPP mode solution and the assistance from a tactical-grade IMU, it was anticipated that the navigation accuracy of the real-time EGI-500 inertial navigation system, under the proposed integration scheme, would fall below 3 meters (the theoretical accuracy of SPP) within this environment. **Figure 10** portrays two trajectories: the red line symbolizes the solution obtained from the reference system, while the purple line represents the solution derived from the EGI-500 system in this study. A numerical analysis revealed that, using the proposed hardware and navigation algorithm integration, the root mean square errors for horizontal and 3D navigation reached 1.284 meters and 1.378 meters, respectively. This level of accuracy is consistent with the "Which Lane" precision target set for this study. Additionally, despite the high dynamics, the root mean square error in velocity remained under 8 cm/s across all directions. This suggests that the navigation solutions were both continuous and suitable for high dynamic situations. Essentially, the proposed integration scheme could effectively estimate the current attitude and determine the attitude angle. Though minor discrepancies in the installation angle within the hardware and on the moving platform were noted, the root mean square errors for the three rotational axes were all below one degree. The accuracy analysis is presented in **Table 4**. The results suggest that, in this type of environment, the integration of hardware and navigation algorithms is practicable for a tactical-grade EGI system.

Figure 10. Trajectory of the open sky experiment

Table 4. Accuracy analysis of proposed system in open sky experiment

Position (m)		
Position Error	2D	3D
Mean Error	1.071	1.224
Max Error	2.729	2.729
Error Std	0.708	0.631
RMSE	1.284	1.378
Velocity (m/s)		
Velocity Error	2D	3D
Mean Error	0.055	0.060
Max Error	0.574	0.577
Error Std	0.048	0.047
RMSE	0.073	0.076

Attitude (degree)			
Attitude Error	Roll	Pitch	Heading
Mean Error	0.650	0.148	0.688
Max Error	0.955	0.311	1.334
Error Std	0.035	0.031	0.395
RMSE	0.651	0.152	0.793

4.2 GNSS Challenging Environments Experiment

The second experimental route traversed an area beneath the bridge piers of the Taiwan High Speed Rail Corporation (THSRC), presenting GNSS challenging environments. Spanning roughly 26 km, the vehicle maintained the speed between 40 and 60 km/h. Like the open-sky experiment, the GNSS solution was set to SPP mode. In **Figure 11**, the reference system solution is represented by the red trajectory, while the purple trajectory illustrates the solution obtained from the EGI-500 system used in this study. Leveraging the SPP mode solution and the tactical-grade IMU, we projected the navigation accuracy of the EGI-500 real-time inertial navigation system to be at the "Which Lane" level within this environment. However, due to the multipath effect, the reliability of the GNSS solutions was impacted. The standard deviation of GNSS solutions was consistently larger than in the open-sky experiment. Consequently, the weighting matrix of GNSS measurements expanded, leading to algorithmic judgment errors. Numerical analysis revealed a maximum horizontal error of 6.689 meters. The accuracy for horizontal navigation and 3D navigation reached only 2.542 meters and 2.757 meters, respectively. Furthermore, the multipath effect also impacted velocity updates, indirectly contributing to errors in attitude angle estimation. Hence, in terms of position, velocity, and attitude, the results were less accurate than those from the open-sky experiment. The accuracy analysis is presented in **Table 5**. Although the accuracy did not reach the "Which Lane" level and remained at the "Which Road" level, this aligned with our expectations. The multipath effect, as previously discussed, complicates the navigation algorithm's calculations. Addressing the multipath issue will require the aid of navigation algorithms. Thus, determining the quality of the GNSS solution will be a critical area for further improvement in the navigation algorithm used in this research.

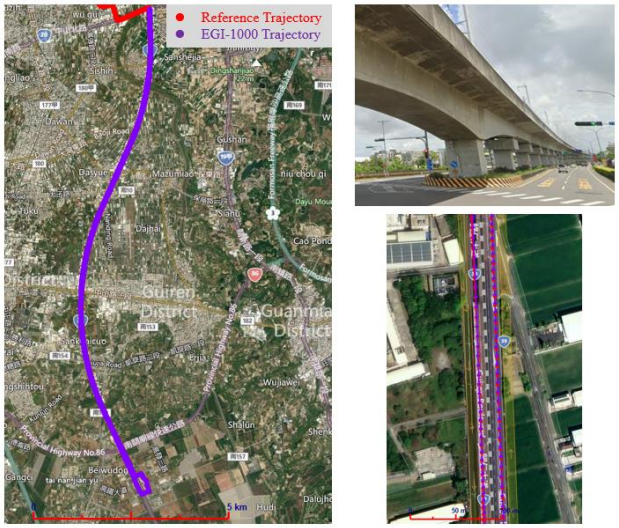

Figure 11. Trajectory of the GNSS challenging environments experiment

Table 5. Accuracy analysis of proposed system in GNSS challenging environments experiment

Position (m)		
Position Error	2D	3D
Mean Error	2.359	2.564
Max Error	6.689	7.460
Error Std	1.882	1.923
RMSE	2.542	2.757
Velocity (m/s)		
Velocity Error	2D	3D
Mean Error	0.181	0.185
Max Error	0.588	0.589
Error Std	0.137	0.135
RMSE	0.227	0.229

Attitude (degree)			
Attitude Error	Roll	Pitch	Heading
Mean Error	0.835	-0.208	0.750
Max Error	1.040	-0.520	1.495
Error Std	0.043	0.045	0.403
RMSE	0.836	0.212	0.851

4.3 GNSS Denied Environments Experiment

The final test route involved navigating a national highway tunnel, a GNSS-denied environment. The tunnel spanned approximately 2.5 km, and the vehicle maintained a steady speed of 80 km/h. Due to the tunnel's obstruction, GNSS connectivity was lost for roughly 112 seconds. As illustrated in **Figure 12**, the red trajectory represents the reference system's solution, whereas the purple trajectory stands for the EGI-500 system's solution. Given the GNSS blockage within the tunnel, the navigation solution had to rely solely on the IMU for inertial navigation. Thanks to the tactical-grade IMU incorporated into our research, we projected that the EGI-500 real-time inertial navigation system under the proposed integration schema should achieve "Which Road" level accuracy in this environment. An effectively estimated IMU-500 error model resulted in a maximum horizontal error of 3.032 m, which was less than the observed error in the GNSS-challenging environment. Moreover, the accuracy in 2D navigation achieved "Which Lane" level with an accuracy of 1.342 m. However, 3D navigation accuracy remained at the "Which Road" level. The accuracy analysis is provided in **Table 6**. In conclusion, despite the unexpected GNSS outage, the methodologies proposed in this study prove their efficacy for

tactical-grade EGI systems, a result surpassing our initial expectations for a GNSS-denied environment.

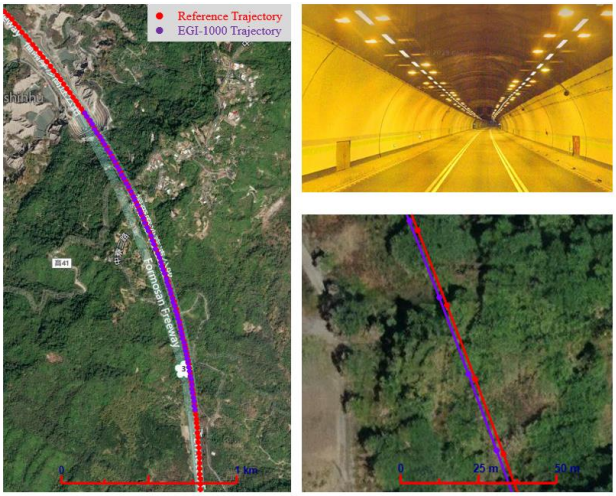

Figure 12. Trajectory of the GNSS denied environments experiment

Table 6. Accuracy analysis of proposed system in GNSS denied environments experiment

Position (m)		
Position Error	2D	3D
Mean Error	1.236	1.236
Max Error	3.032	5.952
Error Std	0.524	1.041
RMSE	1.342	2.366
Velocity (m/s)		
Velocity Error	2D	3D
Mean Error	0.125	0.130
Max Error	0.215	0.216
Error Std	0.053	0.050
RMSE	0.136	0.139

Attitude (degree)			
Attitude Error	Roll	Pitch	Heading
Mean Error	0.834	0.205	0.697
Max Error	0.860	0.240	0.743
Error Std	0.010	0.019	0.022
RMSE	0.835	0.206	0.698

Furthermore, when navigating without any supplementary information to aid the INS, the gyroscopes' bias instability becomes the primary error source, leading to time-dependent drifts (Chuanbin et al., 2004). We use the drift error equation as a benchmark to validate the performance of the developed EGI-500 system. As shown in **Table 7**, both the horizontal and 3D positional errors are lower than the theoretical predictions, indicating the EGI-500's capability to provide plausible solutions. This suggests that the combined hardware and navigation algorithm performs satisfactorily in such environments. However, the discrepancy between the two systems could be attributed to misestimations or other system-level errors in the tactical-grade EGI system. Thus, the next improvement step for the EGI-500 would be to refine the system error estimation process.

$$Error_{b_g} = \frac{1}{6} \times g \times b_g \times t^3 \quad (15)$$

Table 7. Drifting error with 112-seconds in GNSS denied experiment through 2536-meters.

Error (m)	Theoretical maximum errors (m)	Horizontal maximum errors (m)	3D maximum errors (m)
EGI-500	46.681	5.458	5.671
Error drift over the time travelled (TT): 7.8 (cm/s)			
Error drift over the distance travelled (DT): 0.3%			

4.4 Summary

Utilizing the proposed hardware integration and navigation algorithm methodologies in this study, our EGI-500 can attain meter-level precision ("Which Lane" and "Which Road" levels) in open sky, GNSS challenging, and GNSS denied environmental testing. Notably, in GNSS denied scenarios, according to error theory verification, the EGI-500 continues to meet the theoretical standards. This highlights the stability and feasibility of the proposed hardware integration structure and algorithm in terms of navigation performance. Such a system paves the way for an embedded EGI system applicable in land vehicular navigation sectors with stringent accuracy demands.

5. CONCLUSION

This study presents the development of a tactical-grade, real-time integrated navigation system, EGI-500, which encompasses both a hardware architecture and a navigation algorithm. Within the hardware structure, we proposed an architecture that amalgamates a tactical-grade IMU with a GNSS module. This architecture is coupled with a high-precision real-time clock (RTC) chip to maintain accurate time synchronization. Our time synchronization verification approach uses cross-correlation to juxtapose the reference system's IMU data with the test system's IMU data developed in this study. Following the hardware integration phase, the IMU is calibrated to obtain systematic error values, including bias and scale factors. The parameters for the construction of the IMU error model, comprising angular random walk, velocity random walk, and bias instability, are also procured. Utilizing our proposed methods for coarse and fine alignment, we can automatically determine the most opportune time for threshold based on the standard deviation of the stored heading angle values within a one-second period. The integrated algorithm, founded on a loosely coupled scheme, employs an extended Kalman filter for the fusion of IMU and GNSS data. The navigational solutions emanating from the integration of the IMU and GNSS receiver module are obtained using our initial alignment method and motion constraints for auxiliary update observations.

This study executed three distinct experimental setups, employing a ground vehicle as the test platform under three different scenarios: open sky, GNSS challenging environments, and GNSS denied environments. In the open sky testing environment, the root mean square errors for both 2D and 3D were found to be less than 1.5 meters. As per these results, the EGI-500 demonstrated the ability to attain a "Which Lane" level of accuracy in this scenario. The second experiment in GNSS challenging environments resulted in root mean square errors in both 2D and 3D being less than 3 meters. These outcomes suggest that EGI-500 can achieve a "Which Road" level of precision, aligning with the expectation of specific meter-level accuracy in such an environment. Notwithstanding, based on the instrument specifications of EGI-500, we anticipate that the "Which Lane"

level should be attainable in GNSS challenging environments. Thus, future research will need to focus on accurately assessing the quality of the GNSS solution in the algorithm. In the third scenario, a GNSS denied experiment, the error of EGI-500 was in line with the standard of theoretical error as per the error propagation theory of gyro drift rate. However, the actual numerical statistics for 3D navigation accuracy stood at the "Which Road" level. This underscores the need for future research to focus on mitigating positioning error in GNSS denied environments.

6. ACKNOWLEDGMENTS

We extend our deepest gratitude to Yong-Jie Huang, Guang-Je Tsai, Chuan-Te Kuo, Jhih-Cing Zheng, Mei-Chin Hung, and Pei-Ching Hsu for their invaluable assistance throughout this study. Furthermore, we wish to express our appreciation for the financial backing provided by the Ministry of Interior within the Executive Yuan in Taiwan, and for the technical support offered by Gaia Technology. Their contributions have been instrumental in the successful completion of this research.

7. REFERENCES

Petovello, M. G. (2003). “Real-time integration of a tactical-grade IMU and GPS for high-accuracy positioning and navigation (p. 0298)”. *Calgary, AB: University of Calgary, Department of Geomatics Engineering*.

Skog, I., & Handel, P. (2008, May). “Effects of time synchronization errors in GNSS-aided INS”. I*n 2008 IEEE/ION Position, Location and Navigation Symposium (pp. 82-88). IEEE*.

Ferguson, J. (2015). “Calibration of deterministic IMU errors”.

Stephenson, S., Meng, X., Moore, T., Baxendale, A., & Ford, T. (2011, November). Accuracy requirements and benchmarking position solutions for intelligent transportation location-based services. In *Proceedings of the 8th international symposium on location-based services*.

Wang, L., Zhang, C., Lin, T., Li, X., & Wang, T. (2015). “Characterization of a fiber optic gyroscope in a measurement while drilling system with the dynamic Allan variance”. *Measurement, 75, 263-272.*

El-Sheimy, N., Hou, H., & Niu, X. (2007). “Analysis and modeling of inertial sensors using Allan variance”. *IEEE Transactions on instrumentation and measurement, 57*(1), 140-149.

Chuanbin, Z., Weifeng, T., & Zhihua, J. (2004). “A novel method improving the alignment accuracy of a strapdown inertial navigation system on a stationary base”. *Measurement Science and Technology, 15(4), 765*.

Huang, Y. E., Tsai, S., Liu, H. Y., Chiang, K. W., Tsai, M. L., Lee, P. L., & El-Sheimy, N. (2023). “The Development and Validation of a Navigation Grade EGI System for Land Vehicular Navigation Applications”. *The International Archives of the Photogrammetry, Remote Sensing and Spatial Information Sciences, 48, 191-197.*